



Model Investigation of a Cloudband Associated with a Cold Front over Eastern Mediterranean

V. Kotroni, K. Lagouvardos and G. Kallos

University of Athens, Laboratory of Meteorology, Bldg. PHYS-V, 15784 Athens, Greece

Received 26 June 1998; accepted 5 October 1998

Abstract. The aim of this paper is to investigate the occurrence of a cloudband associated with a cold front over the maritime area south from the Greek Peninsula. This cloudband was clearly evident on the infrared satellite picture, oriented nearly parallel to the frontal surface. The relevance of Conditional Symmetric Instability as a possible mechanism for the formation of this band is investigated through model simulations. The model analysis was performed with the three dimensional non-hydrostatic Colorado State University - Regional Atmospheric Modelling System (CSU-RAMS). Inspection of the moist potential vorticity pattern within a cross-section perpendicular to the cloudband supported the hypothesis that Conditional Symmetric Instability was the mechanism which favoured the band formation at the leading edge of the cold frontal surface. © 1999 Elsevier Science Ltd. All rights reserved

1 Introduction

On the 11-12 January 1997 a low pressure system has affected central and south Greece, it was accompanied with a slow-moving cold front and produced heavy rainfall and severe flooding over the area. An interesting feature evident in the satellite imagery was a cloudband associated with the slow moving front. In the frame of this study, the role of Conditional Symmetric Instability (CSI) on the development of the observed cloudband will be investigated through analysis of model results. The model used is the Regional Atmospheric Modelling System (RAMS).

Indeed, the role of CSI in the formation of cloud and/or rain bands has been demonstrated in several studies, based on analysis of observations (e.g. Bennetts and Ryder 1984; Seltzer et al. 1985; Wolfsberg et al. 1986; Lemaître and Scialom 1992, Lemaître and Testud 1988; Lagouvardos et al.

1993). Moreover, numerical analysis studies have provided further evidence on the role that CSI can play in the formation and intensification of banded structure within a convectively unstable region (Knight and Hobbs, 1988).

Section 2 is devoted to a brief synoptic description of the event. Section 3 provides a brief description of RAMS model and the specific settings for the present application. Section 4 is devoted to a brief theoretical presentation of CSI and to the discussion of the role of CSI on the development of the observed cloudband. Some concluding remarks are given in the last section.

2 Synoptic Description

This section provides a short description of the synoptic context within which the cloudband has been formed. The low centre which affected Greece on 11-12 January 1997 has been formed on 9 January over the Gulf of Lion in northwestern Mediterranean (not shown). During the following days this low centre has progressed south-eastward along the west coasts of Italy and on 11 January it is located over Sicily. This is a primary track for cyclones originating from the Gulf of Lion which are then affecting the Ionian Sea (Brody and Nestor, 1980).

At 1200 UTC 12 January 1997, the low centre of 1008 hPa has moved to a position southwest of Greece, approximately at 35°N, 20°E, while the associated cold front has slowly progressed over the area south of Peloponnisos, over Crete and towards the northern African coasts (Fig. 1). The near surface flow ahead of the cold front is intense, presenting a southeastern direction (not shown). This southeastern flow is covering almost the entire part of Eastern Mediterranean. The high pressure system (1039 hPa) located over northeastern Europe extends southwards over the Balkans and it is associated with cold air advection and northeastern surface flow over eastern Balkans and northern Greece. This synoptic setting has been found to favour the eastward propagation of Ionian Sea cyclones across the southern Aegean Sea, instead of a more likely path north-eastwards across Greece (Brody and Nestor, 1980). A more detailed description on the synoptic context of this event is provided in Kotroni et al. (1998).

Correspondance to: Dr. V. Kotroni, University of Athens, Lab. of Meteorology, Panepistimioupolis, Bldg. PHYS-V, 15784 Athens, Greece. E-mail: kotroni@skiron.mg.uoa.gr

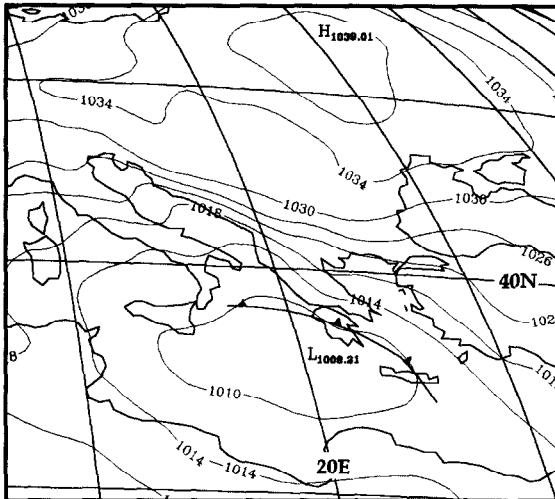


Fig. 1: ECMWF analysis of mean sea-level pressure (at 4 hPa intervals), valid at 1200 UTC 12 January 1997.

The METEOSAT infrared picture at the same time (Fig. 2) shows that over Eastern and Southern Greece, and over southern Aegean Sea a uniform and extended area of convective clouds has developed. The cloud tops are covering a wide area having a northwest-southeast orientation. The edge of the convective clouds over the sea follows very well the cold front analysed at that time on the surface chart (see Fig. 1). A secondary medium level cloud band, approximately 50 km wide, (denoted AB in Fig. 2) is observed at approximately 200-250 km behind the cold frontal position at surface, with a characteristic length of approximately 400 km. Inspection of a serie of METEOSAT images revealed that this cloudband appeared on the images after 0600 UTC, 12 January.



Fig. 2: METEOSAT enhanced infrared-satellite image valid at 1200 UTC 12 January 1997. Letters A and B denote the position of the cloudband.

3 Model Setup

The mesoscale analysis of this case study is based on nested grid simulations performed with RAMS model. A detailed description of the model physics and application fields is given in Pielke *et al.* (1992).

For the present application, RAMS was initialised at 1200 UTC 11 January 1997 and the duration of the simulation was 36 hours. The nonhydrostatic version of the model is employed, while two nested grids have been defined. Indeed the computational domain of the model consists of:

- (a) the outer grid, with a mesh of 76x62 points and 40 km horizontal grid interval centred at 40°N latitude and 20°E longitude
- (b) the inner grid with 122x110 points and 10 km horizontal grid interval, centred at 35° 24' N latitude and 22° 24' E longitude.

The extension of both grids is shown in Fig. 3. Twenty five levels following the topography were used on all grids. The vertical spacing varied from 120 m near the surface to 1 km at the top of the model domain ($z=15.5$ km). Along with these settings, the full microphysical package of RAMS has been activated (Walko *et al.*, 1995); this package includes the condensation of water vapour to cloud water when supersaturation occurs as well as the prognosis of rain, graupel, pristine ice, aggregates, and snow species. Moreover the modified Kuo-type cumulus parametrization developed by Tremback (1990) is used for the outer (40 km) grid, as the model resolved convergence produced at the scales is not enough to explicitly initiate convection.

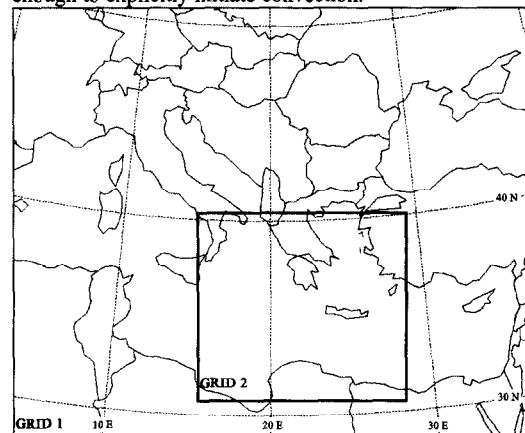


Fig. 3: Horizontal extension of RAMS two nested grids.

The ECMWF 0.5°x0.5° gridded analysis fields are objectively analysed by RAMS model on isentropic surfaces from which they are interpolated to the RAMS grids, and they were used in order to initialise the model and to nudge the lateral boundary region of the RAMS coarser grid. Observed sea-surface temperature data of 1°x1° resolution provided by ECMWF have been used as well as topography derived from a 30"x30" terrain data and gridded vegetation type data of 10"x10' resolution.

4 Model results - CSI Assessment

As it was discussed in section 2, a well defined medium-level cloudband was depicted on satellite imagery on 1200 UTC 12 January, approximately 200-250 km on the rear of the cold

frontal position at surface (denoted AB in Fig. 2). The purpose of this section is to consider the relevance of CSI to the development of this band while the frontal structure is also briefly discussed.

4.1 Theoretical review

A possible explanation for the formation of frontal rainbands is the development of Conditional Symmetric Instability (CSI), proposed by Bennetts and Hoskins (1979). CSI is a form of inertial instability along the equivalent potential temperature surfaces. This type of instability manifests itself by rolls oriented approximately along the vertical shear of the horizontal wind vector (the thermal wind) and bands are generated on the top of the ascending branch of the rolls. A key feature of this theory is the sign of moist potential vorticity (MPV) defined as:

$$\text{MPV} = \left(f + \frac{\partial v}{\partial x} - \frac{\partial u}{\partial y} \right) \frac{\partial \theta_e}{\partial z} \frac{1}{\rho} - \frac{\partial v}{\partial z} \frac{\partial \theta_e}{\partial x} \frac{1}{\rho} + \frac{\partial u}{\partial z} \frac{\partial \theta_e}{\partial y} \frac{1}{\rho}$$

where f is the Coriolis parameter, θ_e the equivalent potential temperature, ρ the air density and MPV is calculated in PVU (Potential Vorticity Units = $\text{m}^2\text{s}^{-1}\text{Kkg}^{-1}$). CSI grows as soon as MPV becomes negative. During the last two decades a considerable number of observational studies demonstrated the role of CSI in the development of cloud and rainbands in a baroclinic atmosphere (a review of observational evidence of CSI can be found in Lagouvardos *et al.*, 1993).

4.2 Horizontal structure of the front

Inspection of RAMS predicted wind patterns revealed that a strong southeastern flow characterises the low-level prefrontal flow. This southeastern flow is predicted over the Eastern Mediterranean and it is extending northwards to the Aegean Sea and the Eastern coasts of Central Greece. At 0000 UTC, 12 January, the most intense winds are predicted over the maritime area north of Crete and they exceed 15 m s^{-1} (not shown). The long path of the air masses over the warm Mediterranean waters supplies them with moisture.

Later on, at 1200 UTC, when the cold front has just crossed the Greek Peninsula, the low-level flow ahead of the frontal discontinuity is from southeast and more intense than 12 hours before, exceeding 18 m s^{-1} northeast of Crete at the 925 hPa level (Fig. 4). The equivalent potential temperature field, at the same level, shows an important horizontal gradient north and south of Crete defining the frontal discontinuity, while ahead of the front a warm conveyor belt is evident with θ_e values exceeding 312 K. As it was mentioned in Kotroni *et al.* (1998) the interaction of this southern flow with the steep topography of Central Greece produced large amounts of precipitation (exceeding 300 mm over 24-hours in some locations over the southern and central part of the country).

4.3 Role of Conditional Symmetric Instability

In order to test CSI, an east-west vertical cross section of θ_e and MPV inside the inner grid of RAMS following approximately the 36°N line (line DD' in Fig. 4) is shown in Fig. 5. The cold front surface is bounded by strong θ_e horizontal gradients, from the ground up to 6 km. As it concerns the moist potential vorticity field, it should be noted, that MPV becomes also negative when the vertical gradient of θ_e is negative. In that case, classical gravitational

instability is developed and therefore CSI is not significant anymore because unstable modes associated with upright convection are growing much faster. For that reason, only the areas where MPV is negative and $\partial\theta_e/\partial z$ is positive (potential instability is inhibited) and hence CSI can grow, are reported in Fig. 5. Inspection of Fig. 5 reveals the existence of a pocket of negative MPV, located within the layer between 2 and 4.5 km, in the warm sector but about 200 km rearwards of the frontal position at surface (denoted by CF in Fig. 5). The cloudband depicted in the infrared satellite picture shown in Fig. 2 is located on the west edge of the pocket of negative MPV, in good agreement with model simulations reported in literature (Knights and Hobbs, 1988; see their Fig. 19).

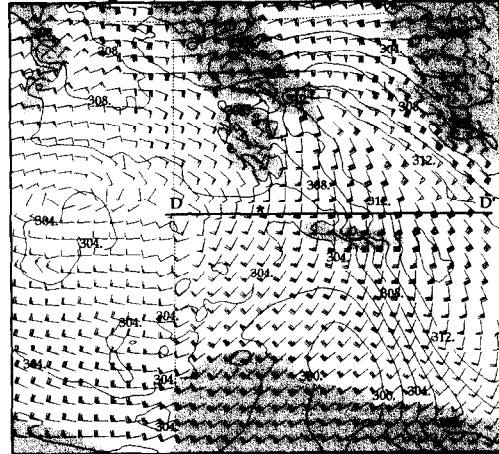


Fig. 4: RAMS inner grid wind and equivalent potential temperature (at 2 K interval) field at the 925 hPa level, at 1200 UTC 12 January 1997. Wind symbols are plotted every fourth grid point (one pennant: 20 m s^{-1} , one barb: 4 m s^{-1} , one half-barb: 2 m s^{-1}). The asterisk denotes the position of the vertical profile used for the construction of the wind hodograph in Fig. 6.

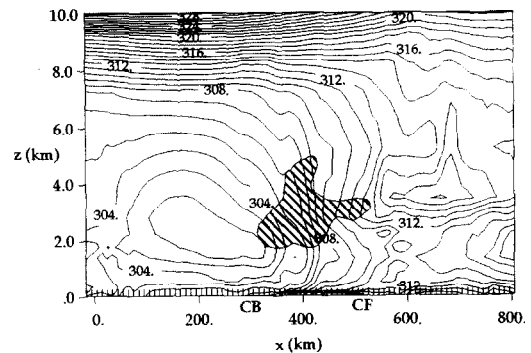


Fig. 5: East-west cross-section of equivalent potential temperature (at 1 K intervals) inside the inner grid of RAMS, following the line DD' shown in Fig. 4, valid at 1200 UTC 12 January 1997. Hatching denotes the area where MPV is negative but the vertical gradient of θ_e is positive (see text for further details). CF and RB denote the position of the cold front at surface and of the CSI rainband, respectively.

The position of a pocket of negative MPV, just ahead of the frontal surface at the mid-tropospheric layers is common in many observational and numerical studies of CSI. Indeed, Lagouvardos *et al.* (1993) estimated MPV from dense upper-air soundings and they showed a similar MPV pattern in the warm sector of a cold front observed during the FRONTS 87

experiment. These findings were also supported by dropsonding analysis over the Atlantic Ocean performed by Thorpe and Clough (1991). Numerical simulations performed by Knight and Hobbs (1988) showed also a pocket of negative MPV on the leading edge of a cold front aloft. According to the authors, this pocket was initially formed in the low-levels ahead of the front and then it was advected upwards from the ascending branch of the secondary ageostrophic circulation developed around the frontal discontinuity.

Wind hodographs are often used in order to determine if the observed cloudbands are parallel to the wind shear vector inside the unstable region as required by CSI theory. A hodograph of the predicted flow from RAMS inner grid has been constructed using a vertical profile in the vicinity of the cloudband location (Fig. 6). Between the heights of 1.7 and 3.4 km and within the unstable layer with respect to CSI (as shown in Fig. 5, in the layer where $\partial\theta_p/\partial z > 0$ and $MPV < 0$) the wind magnitude is increasing while the wind direction does not show much change (ranging from 150 to 160 degrees), and it could be assumed that this is the basic flow within which the CSI flow has been superimposed. The vertical shear within this layer has an orientation of 40 anticlockwise from north while the observed cloudband was aligned almost 30 anticlockwise from north.

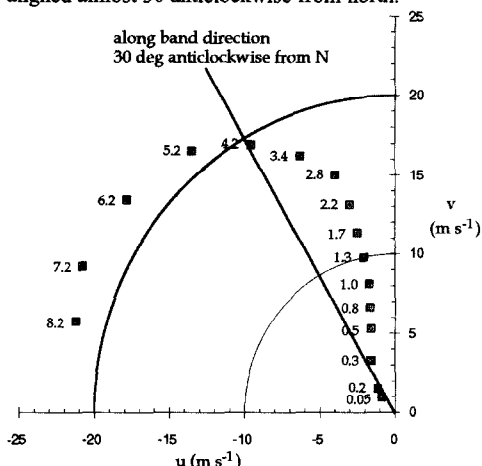


Fig. 6: Wind hodograph constructed from a vertical profile (denoted with an asterisk in Fig. 4) within RAMS inner grid in the vicinity of the observed cloudband. Heights are in kilometres.

This mismatch of a few degrees has been also observed in other studies (Lemaitre and Testud, 1988; Lagouvardos *et al.*, 1993) and it was attributed to the presence of ageostrophic flow around the frontal surface. Thus, the wind hodograph shows that the cloudband was more or less aligned with the wind shear vector in the unstable region, conforming with CSI theory.

5 Concluding Remarks

In the frame of this study the formation of a cloudband, evidenced in the satellite imagery, has been investigated. This cloudband was associated with a cold front which has produced large amounts of rain over central and southern Greece (resulting in a severe flooding). The available data did not permit to conclude if this cloudband evolved into a

rainband, as its path was mainly over a maritime area. The analysis was based on the use of model results provided by the meteorological model RAMS. The cloudband was positioned at an angle of almost 10 degrees from the thermal wind vector inside the unstable layer, which may reflect the influence of ageostrophic circulation. Conditional Symmetric Instability has been examined as a possible mechanism responsible for the formation of the observed cloudband. The band formation was attributed to the onset of CSI. Indeed, the position of the cloudband relative to the surface front, its width, as well as the structure of the moist potential vorticity field suggested that CSI was the physical mechanism which triggered the formation of this band.

Although for the performed simulations the inner grid horizontal increment was 10 km, the obtained results were very encouraging as they reproduced the mesoscale environment within which the cloudband has formed. Radar observation would be necessary in order to comment on the finer scale circulations associated with the cloudband. These kind of data are not available over the area and thus a meteorological model such as RAMS consists an important tool for such type of studies.

Acknowledgements. The authors are grateful to the Hellenic National Meteorological Service and especially to Mr. G. Potiriadis for providing the METEOSAT data used in this study.

References

- Bennetts, D.A. and B. J. Hoskins, Conditional Symmetric Instability - a possible role for frontal rainbands. *Q. J. R. Meteor. Soc.*, 105, 945-962, 1979.
- Bennetts D.A. and Ryder, P., A study of mesoscale convective bands behind cold fronts. Part I: Mesoscale organisation. *Q. J. R. Meteor. Soc.*, 110, 121-145, 1984.
- Brody, L.R. and Nestor, M.J.R., Regional forecasts for the Mediterranean basin. Technical report n° 80-10, Naval Environmental Prediction Research Facility, Monterey California, pp. 178, 1980.
- Knight, D.J and Hobbs, P.V., The mesoscale and microrcale structure and organization of clouds and precipitation in midlatitude cyclones. Part XV: a numerical modeling study of frontogenesis and cold-frontal rainbands. *J. Atmos. Sci.*, 45, 915-930, 1988.
- Kotroni V., Lagouvardos, K., and Kallos, G., Dynamics of a cold front associated with heavy precipitation over eastern Mediterranean, *Q. J. R. Meteor. Soc.* (in press), 1998.
- Lagouvardos, K., Lemaitre, Y., and Scialom, G., Dynamical structure of a wide cold-frontal cloudband observed during FRONTS 87. *Q. J. R. Meteor. Soc.*, 119, 1291-1319, 1993.
- Lemaitre, Y. and Scialom, G., Three dimensional mesoscale circulations within a convective post-frontal system. Possible role of conditional symmetric instability for triggering convective motion. *Q. J. R. Meteor. Soc.*, 118, 71-99, 1992.
- Lemaitre, Y. and Testud, J., Relevance of conditional symmetric instability in the interpretation of wide cold-frontal rainbands. A case-study 20 May 1976. *Q. J. R. Meteor. Soc.*, 114, 259-270, 1988.
- Pielke, R.A., Cotton, W.R., Walko, R.L., Tremback, C.J., Lyons, W.A., Grasso, L.D., Nicholls, M.E., Moran, M.D., Wesley, D.A., Lee, T.J., and Copeland, J.H., A comprehensive meteorological modelling system - RAMS. *Meteorol. Atmos. Phys.*, 49, 69-91, 1992.
- Seltzer, M.A., Passarelli, R.E., and Emanuel, K.A., The possible role of symmetric instability in the formation of precipitation bands. *J. Atmos. Sci.*, 42, 2207-2219, 1985.
- Thorpe A.J., and Clough, S.A., Mesoscale dynamics of cold fronts. I Structures described by dropsondings in FRONTS 87. *Q. J. R. Meteor. Soc.*, 117, 903-941, 1991.
- Tremback, C. J., Numerical simulation of a mesoscale convective complex: Model development and numerical results. Ph.D. dissertation, Atmos. Sci. Paper No. 465, Colorado State University, Dept. of Atmos. Science, Fort Collins, Co 80523, 1990.
- Walko, R.L., Cotton, W.R., Meyers, M.P., and Harrington, J.Y., New RAMS cloud microphysics parameterization. Part I: the single moment scheme. *Atmos. Res.*, 38, 29-62, 1995.
- Wolfsberg, D.G., Emanuel, K.A., and Passarelli, R.E., Band formation in a New England winter storm. *Q. J. R. Meteor. Soc.*, 115, 1325-1353, 1986.